JOURNAL OF SOLID STATE CHEMISTRY 53, 101–112 (1984)

Oxidation of Bismuth–Tungsten Bronzes

D. A. JEFFERSON AND M. K. UPPAL

Department of Physical Chemistry, Lensfield Road, Cambridge CB2 1EP, United Kingdom

AND DAVID J. SMITH

High Resolution Electron Microscope, University of Cambridge, Free School Lane, Cambridge CB2 3RQ, United Kingdom

Received October 14, 1983; in revised form January 16, 1984

The oxidation of bismuth–tungsten bronzes at 600 and 950°C has been studied using high-resolution electron microscopy at 200 and 500 kV. At the lower temperature, a topotactic transformation to lamellae of Bi_2WO_6 in a WO_3 matrix was observed but at higher temperature larger crystals were produced, primarily of $Bi_2W_2O_9$ but with some disordered intergrowths.

Introduction

Bismuth tungstates form a potential homologous series of general formula $Bi_2W_nO_{3n+3}$, the structural principles of this series being indicated in Fig. 1. The different structures are examples of Aurivillius phases (1) formed by intergrowth of layers of BiO with n layers of a perovskite phase ABO_3. In the case of the bismuth tungstates however, the A sites of the perovskite component are left empty. The first two members have been characterized in well crystalline form, using neutron diffraction and high resolution electron microscopy (HREM), respectively (*2, 3*) but attempts to prepare higher members of the series have been inconclusive. Disordered intergrowths of the $n = 3$ phase have been reported (*4*) but these were found to revert, upon subsequent annealing, to $Bi_2W_2O_9$ and WO_3 (*5*). Unlike the molybdenum analog, $Bi_2Mo_3O_{12}$, which has a scheelite-derived structure (*6*), the $n = 3$ member of the tungstate series retained the layered form, suggesting that more complex layered structures may exist in metastable form.

One possible method of preparing phases with $n \geq 3$ is by the oxidation of reduced Bi–W–oxides with low Bi content. These constitute the Bi–W–bronzes of general formula Bi_xWO_3. Powder X-ray diffraction studies have indicated that these belong to the intergrowth tungsten bronze (ITB) family of structures and preliminary HREM studies (*7*) revealed a close similarity to Pb_xWO_3 (*8*), in which the nature of the intergrowth has not been defined. More detailed HREM work (*9*), however, has revealed that Bi_xWO_3 has a structure similar to those of Rb_xWO_3 and Cs_xWO_3 (*10, 11*), with strips of hexagonal tungsten bronze (HTB) separated by slabs of WO_3. In the Bi–bronzes, the HTB strips are invariably

0022-4596/84 $3.00

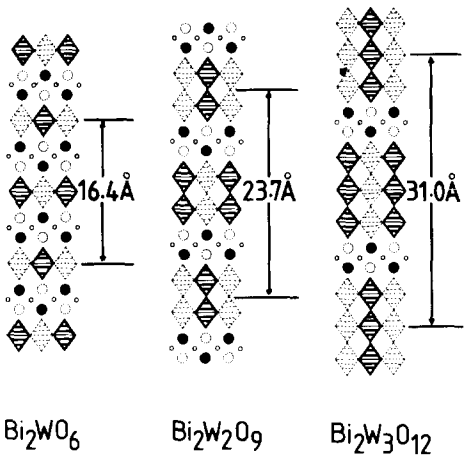

FIG. 1. Idealized structural arrangement of the first three members of the $Bi_2W_2O_{3n+3}$ series, projected down [100].

only one unit wide, and the hexagonal tunnels are fully occupied, making their identification difficult at all but the highest resolution. A schematic structural diagram and HREM image of a nominal $Bi_{0.1}WO_3$ are shown in Fig. 2. The study described here was an attempt to investigate the oxidation and decomposition of these bronzes over a range of temperatures. A preliminary report of some of this work has been published elsewhere (*12*).

Experimental

Samples of Bi_xWO_3 (with nominal values of 0.02, 0.05, 0.1, and 0.2) were prepared by direct combination of metallic Bi and WO_3 in evacuated silica tubes at 900°C. This was followed by further annealing in sealed tubes for up to 6 days at 600°C. Portions were oxidized by heating in air at 600°C for periods of 1 to 5 hr, and at 950°C for slightly longer periods. Some loss of WO_3 by evaporation was noted at the higher temperatures.

All samples were characterized using selected area electron diffraction (SAED) and HREM imaging. Initial examination was carried out on a JEM-200CX fitted with a side-entry goniometer (C_s = 1.9 mm) operating at 200 kV. The interpretable point resolution of *ca* 2.8 Å at the Scherzer focus in this configuration was barely adequate to characterize the disordered $Bi_2W_nO_{3n+3}$ phases formed, and samples oxidized at the higher temperature were examined in the Cambridge University HREM (*13*) at 500 kV. The objective lens characteristic of this instrument (C_s = 2.7 mm) was such that the interpretable resolution could be extended to *ca*. 2.0 Å, and image interpretation could be carried out intuitively in thin regions of crystals. For the lower-resolution studies, computer-simulation of images was performed using the multi-slice method (*14*) using programs modified to deal with defect crystals. Simulation of perfect and defect crystal images confirmed that local lattice periodicity could be used to characterize the member of the $Bi_2W_nO_{3n+3}$ series within 300 and 400 Å of the Scherzer focus.

Results

The general appearance of crystals of a sample of nominal composition $Bi_{0.1}WO_3$ after 2 hr oxidation at 600°C is shown in Fig. 3. Figure 3a shows that the initial bronze structure still predominates, but nuclei of a second phase are present, although not at the crystal edges. This second phase, which occurred in both lamellar and equidimensional morphology, showed a characteristic fringe spacing of *ca*. 8 Å, these fringes being either parallel with, or perpendicular to, the HTB strips of the Bi–bronze. The SAED pattern of the same crystal (Fig. 3b) shows clear maxima from this second phase and, although relatively diffuse, these spots corresponded with those expected from a structure in the $Bi_2W_nO_{3n+3}$ series, with Bi_2WO_6 as the strongest possibility.

After further oxidation, growth of nuclei was observed, and considerable regions of

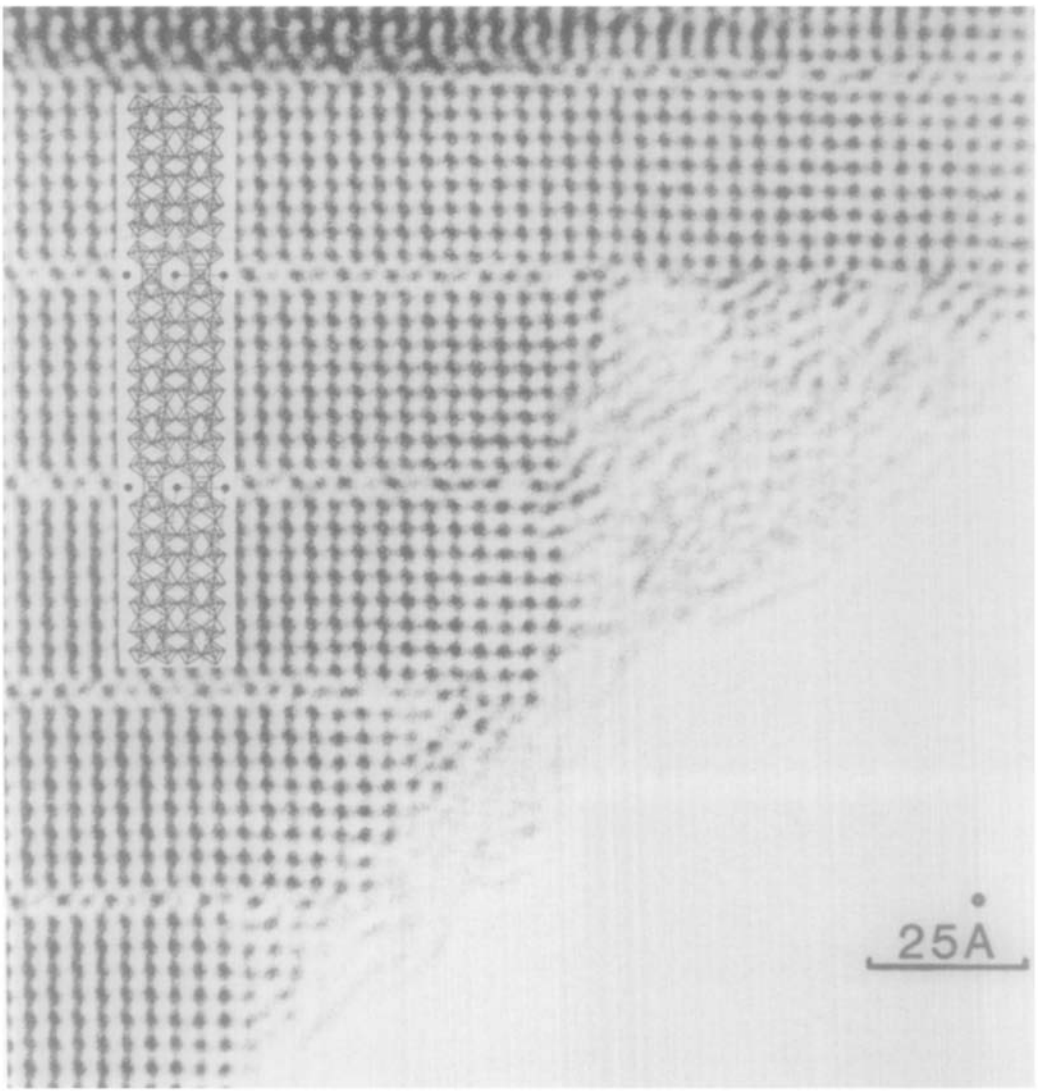

FIG. 2. HREM image of a Bi–W–bronze of nominal composition $Bi_{0.1}WO_3$ taken at 500 kV, with a diagrammatic representation of the structure. The electron beam is parallel to the axis of the hexagonal tunnels.

WO_3 intruded into the Bi–W–bronze matrix, as shown in Fig. 4a. Where the density of nuclei was large, holes were observed together with severely disordered regions (Fig. 4b). Apart from the gradual replacement of the Bi–W–bronze by WO_3 as matrix phase, little alteration of the crystal margins was observed except in a few regions where the WO_3 slabs appeared to be associated with some quasi-amorphous material (Fig. 5). With prolonged oxidation, the Bi–W–bronze phase disappeared completely, and a distinctive recrystallization of nuclei was observed. These invariably became of lamellar-like form, generally of sub-50 Å width, but extending completely across the crystals within which they occurred. These lamellae were separated by

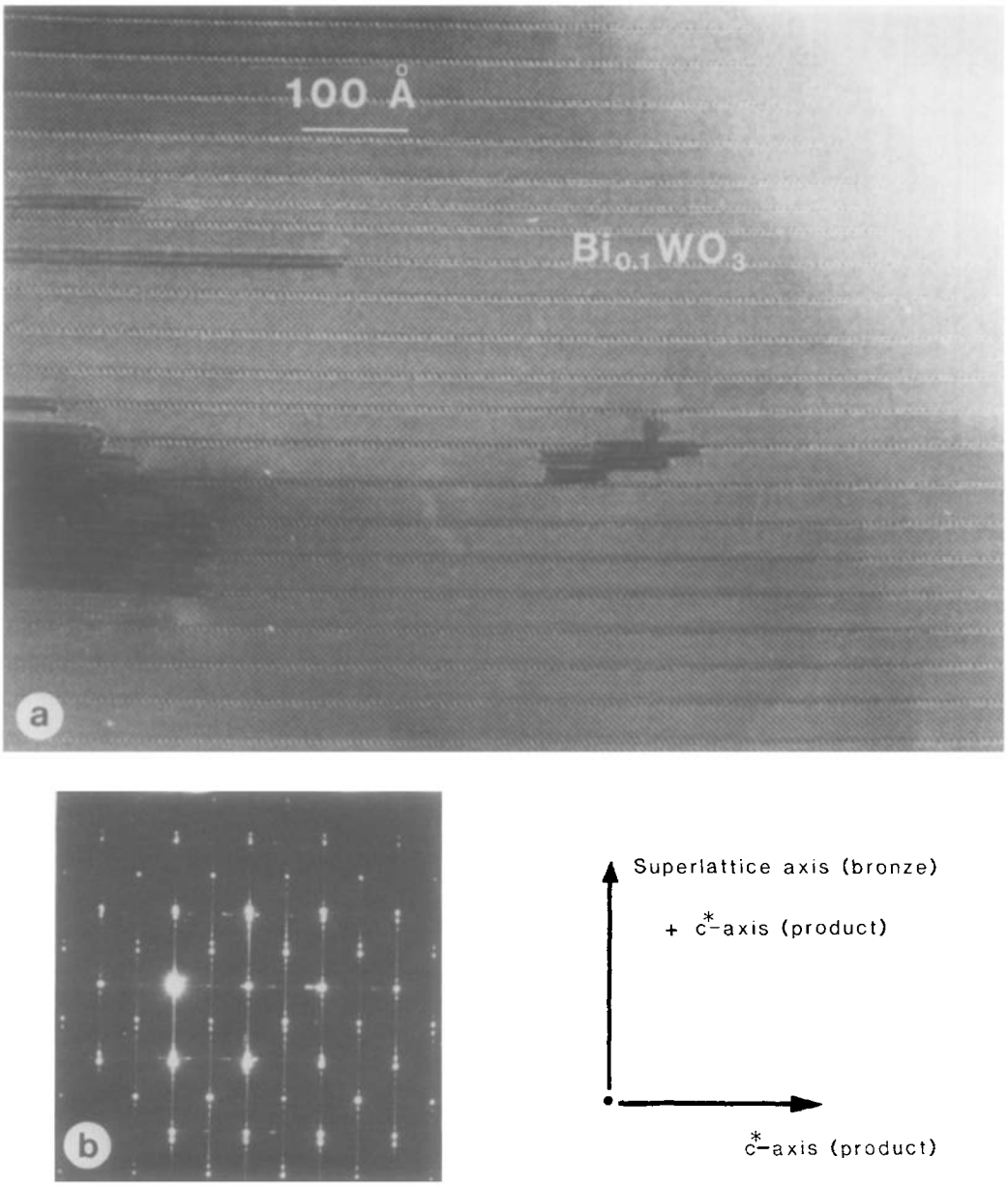

FIG. 3. (a) HREM (200 kV) image of a crystal of $Bi_{0.1}WO_3$ after 2 hr oxidation at 600°C. The electron beam is parallel to the tunnel axis of the bronze structure. (b) The corresponding SAED pattern, showing diffraction maxima from the oxidized phase which are striated in a direction perpendicular to the superlattice of the Bi–W–bronze.

WO_3 regions of at least 100 Å width, as shown in Fig. 6a. The periodicity within lamellae was measured as 8.2 Å, corresponding to the layer thickness of Bi_2WO_6. Image matching studies (Fig. 6b), showed that the observed image contrast was compatible with that expected from the Bi_2WO_6 structure, but the overall level of the observed

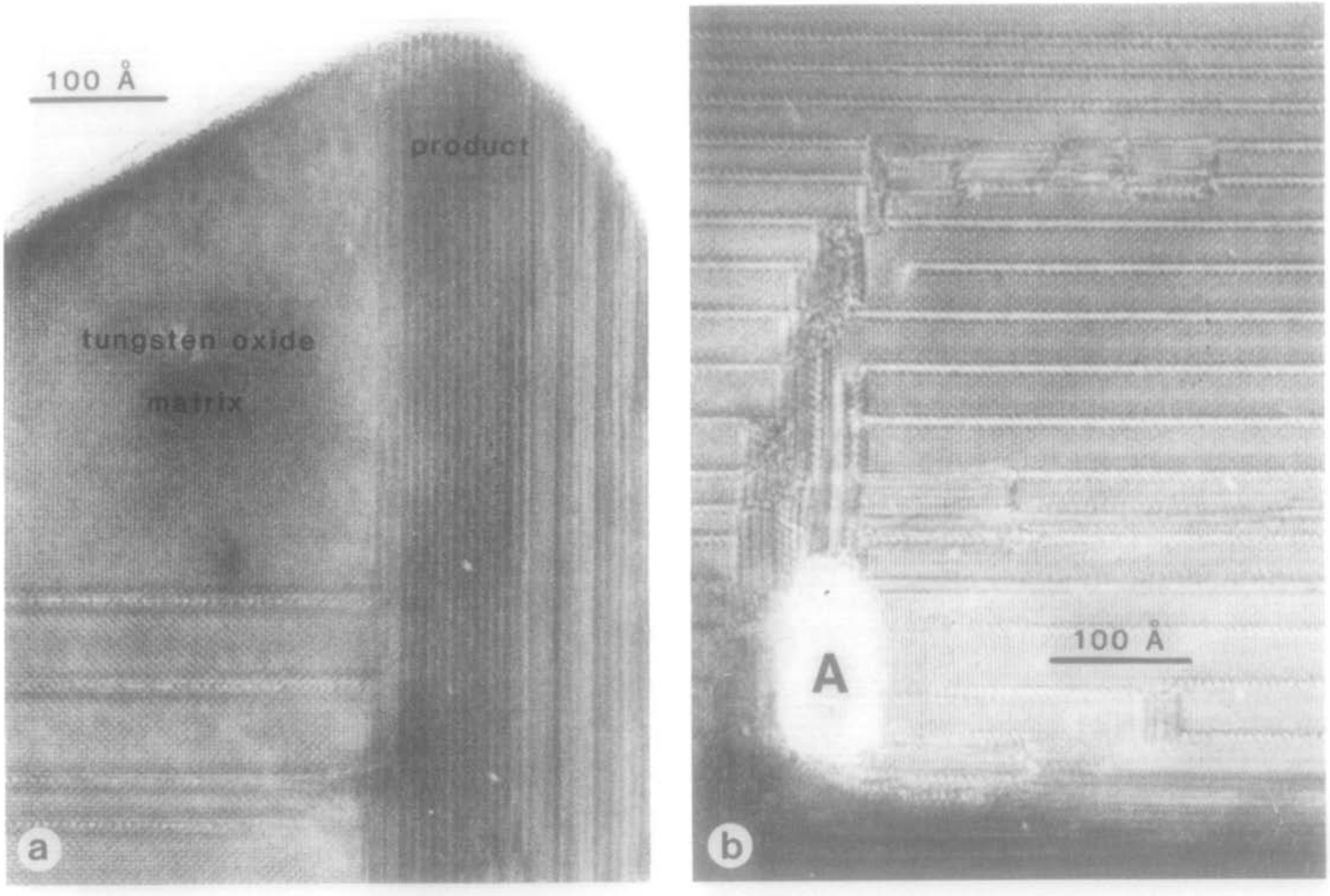

FIG. 4. (a) Image (200 kV) showing the development of extensive areas of pure WO_3 matrix. (b) A severely disordered region, with the bronze structure predominating, but with a hole (A) developed in the crystal lattice.

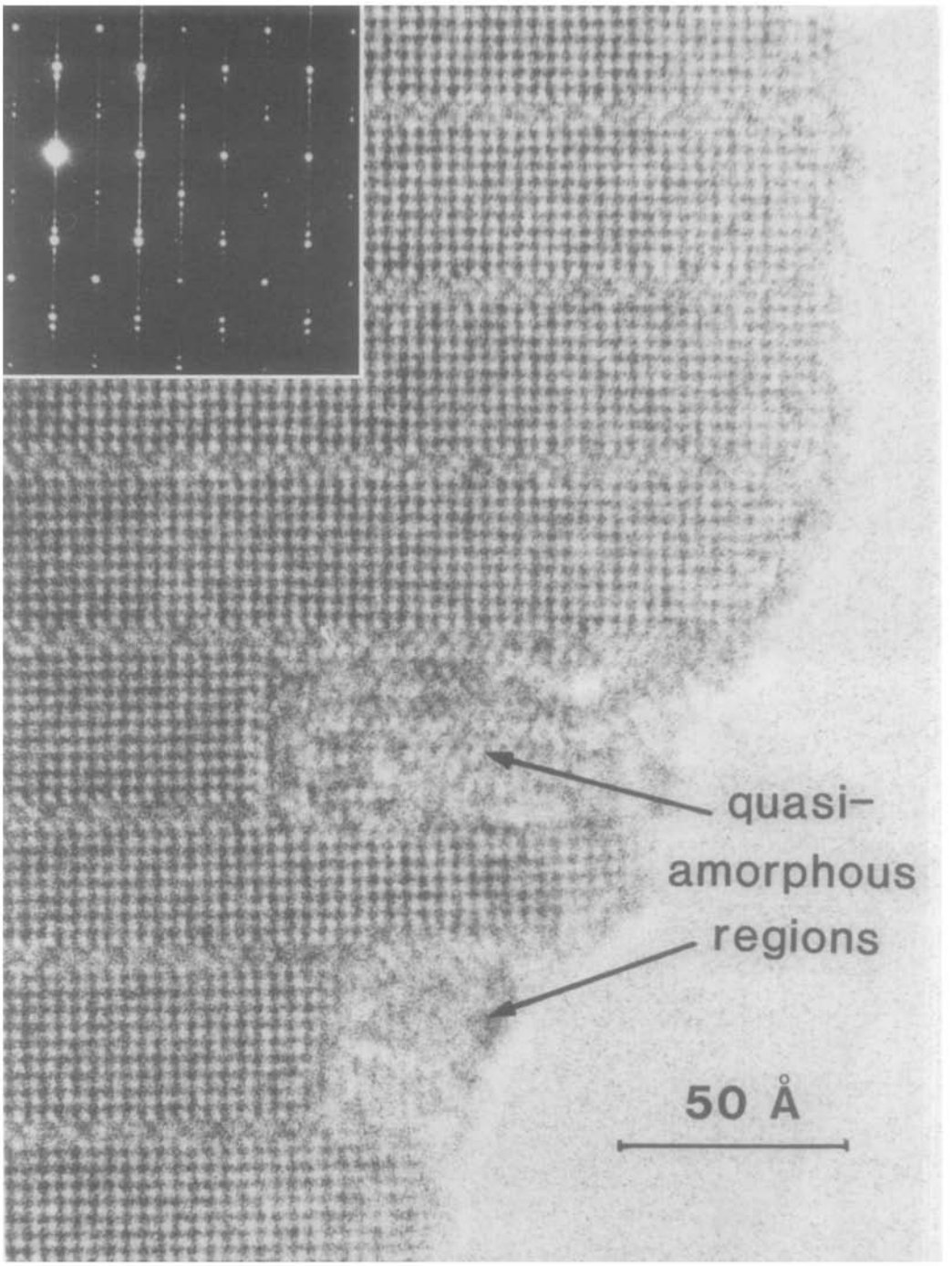

FIG. 5. Image (200 kV) of the edge of a crystal of untransformed bronze, showing quasi-amorphous regions (indicated).

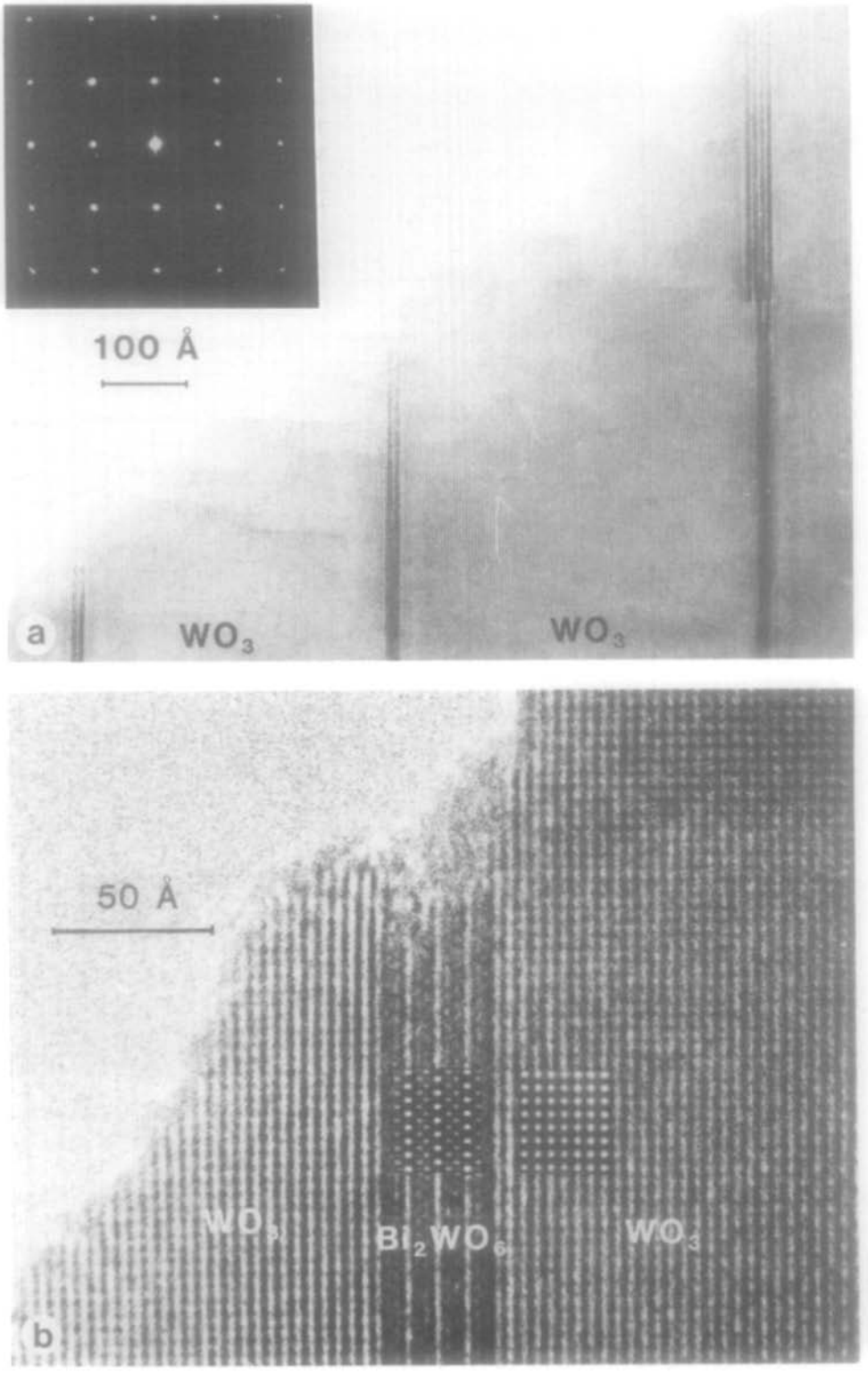

FIG. 6. (a) Image (200 kV) of a crystal of $Bi_{0.1}WO_3$ after 5 hr oxidation at 600°C, showing lamellae. (b) A region of (a), with an image match for the Bi_2WO_6 lamellar structure. The conditions of the computer simulation were: defocus −900 Å, crystal thickness, 45 Å; C_s, 1.9 mm; axis of projection [110].

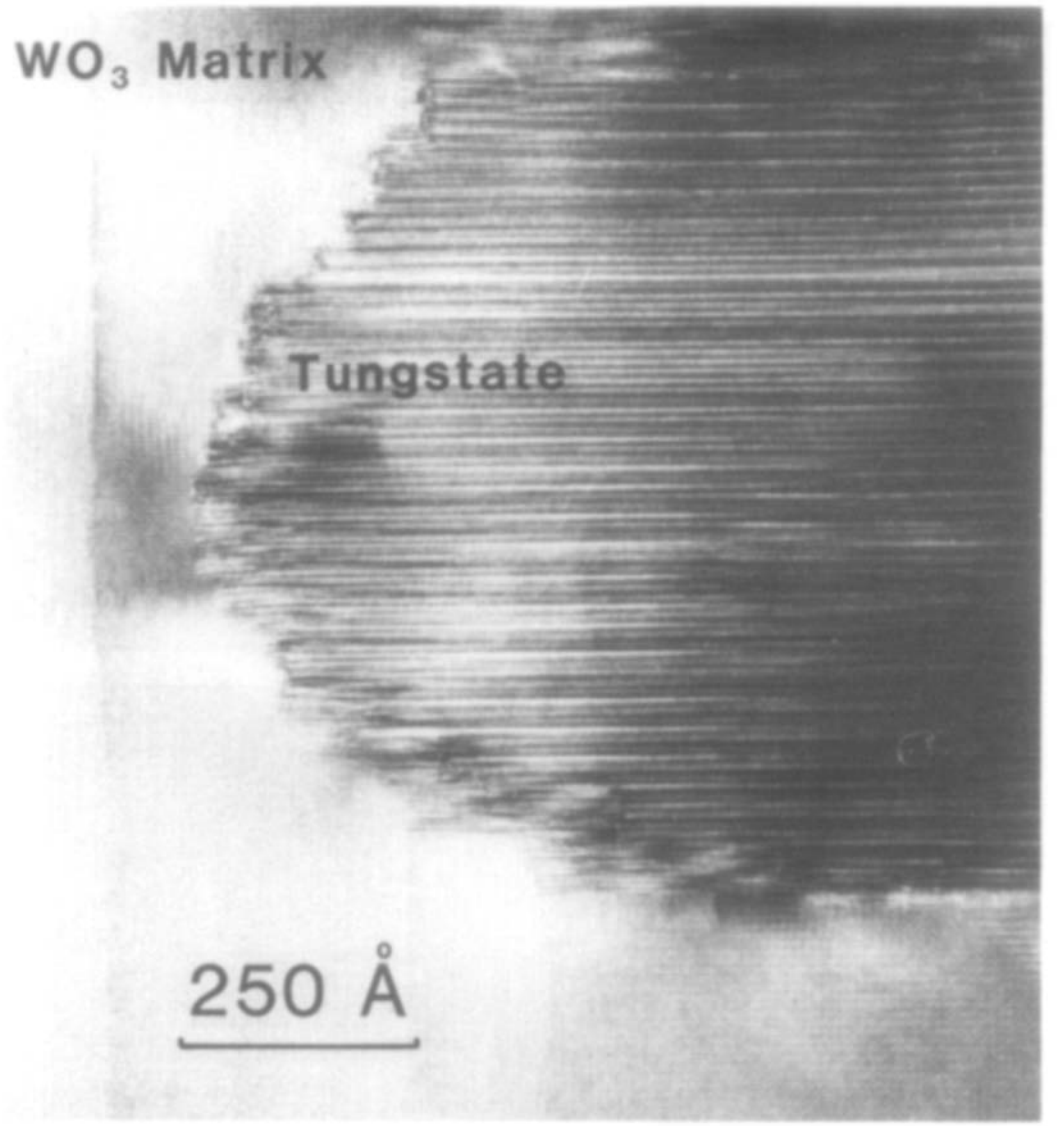

FIG. 7. Image (500 kV) of a crystal of $Bi_{0.2}WO_3$ after oxidation at 950°C, showing a disordered tungstate crystallite within a WO_3 matrix.

contrast was lower than that of the simulation, implying that microscope chromatic and beam divergence effects were slightly greater than those given by the manufacturer.

For samples oxidized at 600°C, the ultimate product was Bi_2WO_6, irrespective of the original composition, and little or no disorder was observed in the tungstate phase produced. At 950°C, however, the fi-

FIG. 8. (a) Image (500 kV) of a crystal of $Bi_2W_2O_9$ produced by the oxidation of $Bi_{0.2}WO_3$ at 950°C. (b) Image of a similar crystal, showing considerable disorder. Schematic structural models are indicated and the electron beam is parallel to [110] in both cases.

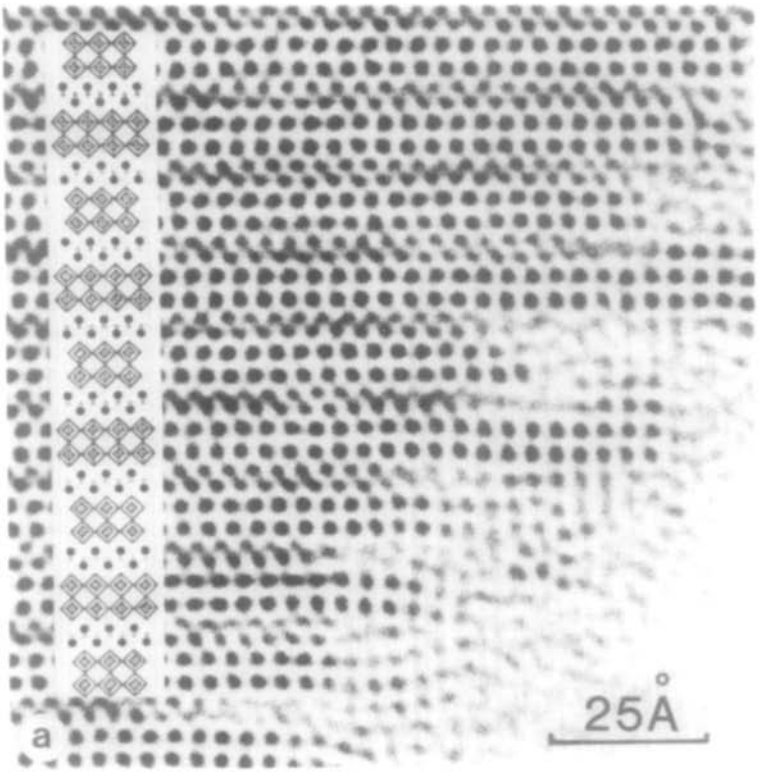
25Å
a

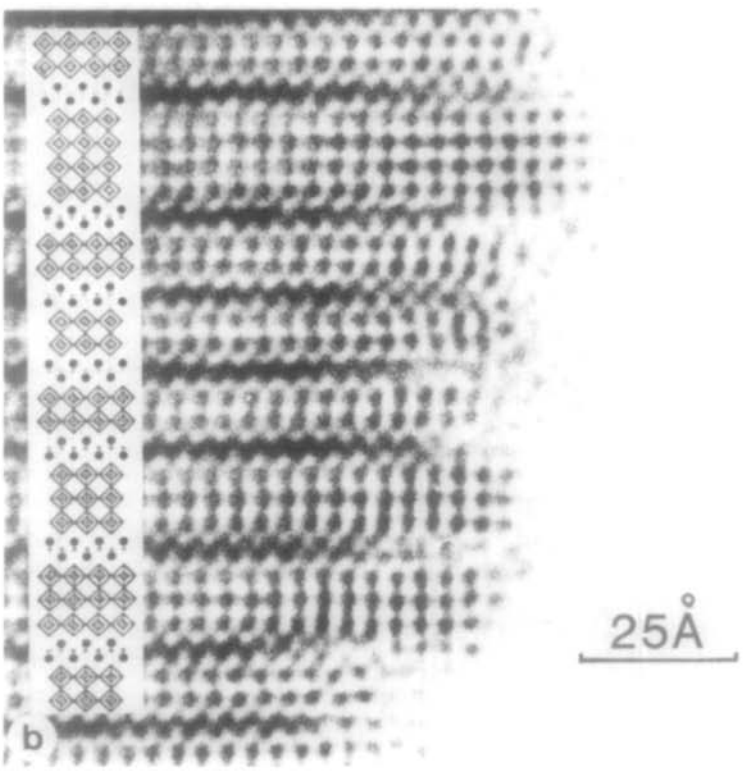
25Å
b

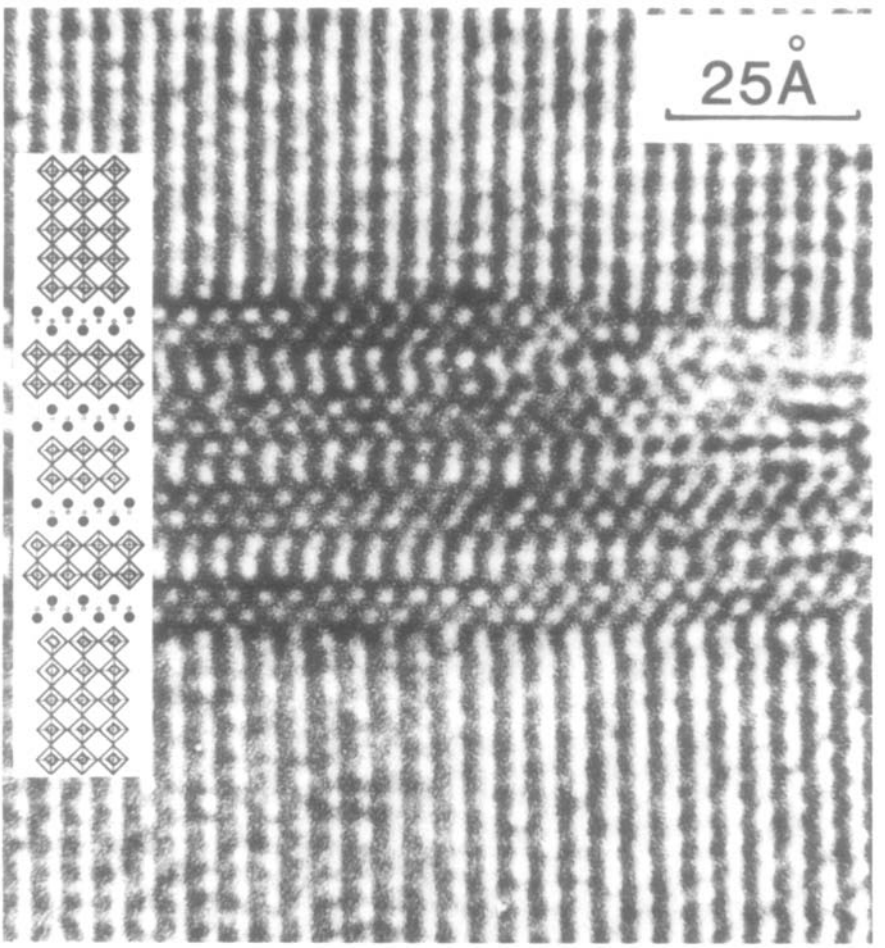

FIG. 9. Image (500 kV) of a thin lamella of $Bi_2W_2O_9$ in a WO_3 matrix.

nal oxidation product was less well-defined, with relatively large nuclei being generated, showing considerable disorder. On prolonged treatment, these grew in size to give crystals of a tungstate product in a WO_3 matrix, as indicated in Fig. 7, with some lamellae being observed also. The predominant phase produced was $Bi_2W_2O_9$, which occasionally occurred in well-ordered crystals such as that illustrated in Fig. 8a. Other crystals, however, showed intergrowths of different members of the series, a typical example being that of Fig. 8b, where regions of $n = 3$ tungstate are evident, and a unit cell strip of the $n = 4$ member. Unit cell strips with n values of up to 10 were noted, but these always occurred singly. Some lamellar product was observed, generally in the thicker crystals, and these could be identified by lattice spacing as consisting of $Bi_2W_2O_9$. One such lamella is shown in Fig. 9, although the regular $Bi_2W_2O_9$ structure is not maintained at the very edge of the crystal, as indicated by the narrowing of the lamella at the right-hand side of the micrograph. This is almost certainly due to the existence of a quasi-reduced phase in the very thin regions of the crystals, as has

been observed previously (*3*). Reduction of the matrix was also noticed occasionally, with various configurations of crystallographic shear (*CS*) planes being observed. In no case, however, was there any indication of ordered *CS* structures being formed.

Discussion

At the lower temperature (600°C) the oxidation process shows the classical behavior of a solid-state reaction initiated well away from the equilibrium *P/T* curve with the large free energy difference giving rise to very many nuclei. Oxidation must occur at the crystal edges, accompanied by migration of Bi atoms in the crystal centers and movement of W atoms in the opposite direction. Development of the tungstate product exclusively at the crystal edges was never observed, even when specimens were ground up prior to oxidation and received no further mechanical treatment before HREM examination. Consequently the natural tendency to develop the fully oxidized phase (i.e., the Bi-tungstate) at the surface, where oxygen availability is maximized, must be offset by the even greater ease of WO_3 formation. Features of the type shown in Fig. 5 may represent the development of fresh WO_3 at the crystal edges, although they were only infrequently observed. The tunnels in the original bronze structure were more clearly defined in the partly oxidized samples, suggesting that some Bi had been abstracted to form the tungstate nuclei. But, although it is logical to suppose that Bi atom migration (and that of W atoms) is facilitated along the length of the tunnels, there was no conclusive evidence to indicate the preferential formation of lamellar nuclei in a direction perpendicular to these tunnels. In the initial stages of the reaction the migration of W atoms appears to outstrip that of Bi: this could account for the holes observed in the centers of most crystals.

Initially, nuclei form equally in all three dimensions, but when oxidation nears completion, and growth of nuclei commences, considerations of lattice mismatch then appear to become paramount. The unit cell dimensions of WO_3 (*15*) differ quite considerably from the corresponding distances within the octahedral component of a $Bi_2W_nO_{3n+3}$ layer ($1 \rightarrow 6\%$) but the difference is far greater when the tungstate repeat perpendicular to the layers is considered ($7 \rightarrow 12\%$). Consequently, lattice mismatch, and the associated strain energy, will be minimized if the tungstate nuclei are converted into lamellar form with the plane of contact between tungstate and WO_3 matrix being (001). This is invariably observed in practice when oxidation is carried out at 600°C, and no separate crystals of Bi_2WO_6 are formed.

At the higher oxidation temperature (950°C) the nuclei of tungstate tended to be larger, suggesting that they form more slowly. In general there appears to be far less energetic preference for a particular tungstate structure, as shown by the much more disordered nature of the nuclei, and this disorder may help to alleviate the strain energy incurred when the nuclei and matrix meet along other than the (001) planes. Once the nuclei reach a certain size, they appear to form completely incoherent boundaries with the associated WO_3, and can be regarded as separate crystals. It is significant that lamellar-like structures of the type shown in Fig. 9 were only observed when the actual amount of $Bi_2W_2O_9$ produced, and consequently the lamellar thickness, was quite small. The higher temperature results, therefore, are fully consistent with conversion to a product phase nearer the equilibrium curve, where nuclei can readily grow by diffusion and constitute a true second phase, rather than the coher-

ent intergrowth obtained at the lower oxidation temperature.

The variation of the nature of the product phase with temperature is also significant, suggesting that the only truly stable low-temperature phase is Bi_2WO_6. At higher temperatures, $Bi_2W_2O_9$ is favored if the composition is suitable and, indeed, even single unit cell intergrowths of the former were not observed at 950°C. Whether the $n \geq 3$ members of the series are ever thermodynamically stable at temperatures near the melting point remains enigmatic, since energy differences between them might be expected to be small, and more than offset by the entropy factors resulting from disordered intergrowths which were obtained.

Conclusions

The experimental results are in accordance with accepted theories of solid state transformations, and indicate that sub-solidus preparation of higher members of the $Bi_2W_2O_{3n+3}$ homologous series is not possible except in disordered form. They also confirm previous hypotheses that the more complex structures are only stable at higher temperatures. Further work on these phases, particularly their relationship to molybdenum analogs (*16*), is continuing.

Acknowledgments

We acknowledge the advice and encouragement of Professor C. N. R. Rao, who provided the original samples of Bi_xWO_3. D. J. S. and M. K. U. acknowledge financial support from the SERC.

References

1. B. AURIVILLIUS, *Ark. Kemi* **1,** 463 (1949).
2. S. N. HODA AND L. L. Y. CHANG, *J. Amer. Ceram. Soc.* **57,** 323 (1974).
3. Y. BANDO, A. WATANABE, Y. SEKIKAWA, M. GOTO, AND S. HORIUCHI, *Acta Crystallogr. Sect. A* **35,** 142 (1979).
4. D. A. JEFFERSON, J. GOPALAKRISHNAN, AND A. RAMANAN., *Mater. Res. Bull.* **17,** 269 (1982).
5. D. A. JEFFERSON, *Philos. Trans. Roy. Soc. London Ser. A* **305,** 535 (1982).
6. A. F. VAN DER ELZEN AND G. D. RIECK, *Acta Crystallogr. Sect. B* **29,** 2433 (1973).
7. D. A. JEFFERSON, M. K. UPPAL, J. GOPALAKRISHNAN, A. RAMANAN, AND C. N. R. RAO, "Proceedings, 2nd European Conference on Solid State Chemistry, Eindhoven (1982)."
8. T. EKSTROM AND R. J. D. TILLEY, *J. Solid State Chem.* **24,** 209 (1978).
9. D. A. JEFFERSON, M. K. UPPAL, D. J. SMITH, AND C. N. R. RAO, *Mater. Res. Bull.*, in press.
10. A. HUSSAIN, *Chem. Scr.* **11,** 224 (1977).
11. L. KIHLBORG, *Chem. Scr.* **14,** 187 (1979).
12. D. A. JEFFERSON AND D. J. SMITH. *in* "Proceedings, 7th International Conference on High Voltage Electron Microscopy (Berkeley)" (R. M. Fisher, R. Gronsky and K. H. Westmacott, Eds.), pp. 385–388, Lawrence Berkeley Laboratory, Berkeley (1983).
13. D. J. SMITH, R. A. CAMPS, L. A. FREEMAN, R. HILL, W. C. NIXON, AND K. C. A. SMITH, *J. Microsc.* **130,** 127 (1983).
14. P. GOODMAN AND A. F. MOODIE, *Acta Crystallogr. Sect. A* **30,** 280 (1974).
15. B. O. LOOPSTRA AND P. BOLDSINI, *Acta Crystallogr.* **21,** 158 (1966).
16. D. A. JEFFERSON, J. M. THOMAS, M. K. UPPAL, AND A. K. GRASSELLI, *J. Chem. Soc. Chem. Commun.* 594 (1983).